UCRL-9967 Rev.

University of California

Ernest O. Lawrence Radiation Laboratory

Berkeley, California

DISCLAIMER

Submitted to Health Physics

UCRL-9967 Rev.

UNIVERSITY OF CALIFORNIA
Lawrence Radiation Laboratory
Berkeley, California

Contract No. W-7405-eng-48

NEUTRON DOSIMETRY IN AND AROUND HUMAN PHANTOMS BY USE OF NUCLEAR TRACK EMULSION

Hiroaki Akagi
Richard L. Lehman

April 1962

UCRL-9967 Rev.

NEUTRON DOSIMETRY IN AND AROUND HUMAN PHANTOMS BY USE OF NUCLEAR TRACK EMULSION

Hiroaki Akagi and Richard L. Lehman

Lawrence Radiation Laboratory
University of California
Berkeley, California

April 1962

Abstract

The validity of the nuclear track emulsion technique for fast-neutron dosimetry is examined in the exposure of a human phantom to PuBe neutrons. Semiautomatic track scanning and high-speed data analysis obviate the major disadvantages of emulsion dosimetry, and allow the absolute differential proton track energy spectrum, at various locations in the phantom to be obtained without a serious cost in time. From this are calculated the total absorbed local tissue dose due to proton recoils and the local thermal neutron intensity during irradiation.

NEUTRON DOSIMETRY IN AND AROUND HUMAN PHANTOMS BY USE OF NUCLEAR TRACK EMULSION

Studies with Plutonium-Beryllium Neutrons

Hiroaki Akagi and Richard L. Lehman

Lawrence Radiation Laboratory
University of California
Berkeley, California

April 1962

I. INTRODUCTION

Nuclear track emulsion has been widely used for detection and measurement since the beginning of neutron research. However, health physicists have not until now shown much interest in this tool, which is probably the best single neutron dosimeter. The reason for this lack of interest is simple: track scanning and analysis require a great deal of time. Now semi-automatic scanning of emulsions and data analysis by electronic computer have partly overcome this difficulty. But the question arises – "How good is this tool for analyzing and evaluating tissue dose from neutron exposure?"

In an attempt to answer this question, nuclear track emulsion was exposed in and around human phantoms to various kinds of neutrons. In this report we present data obtained from exposure to plutonium-beryllium neutrons. These data include the absolute differential energy spectra, average energy, and emulsion dose of proton tracks at various depths in the phantom. From this the tissue dose is calculated.

II. EXPERIMENTAL METHOD

The nuclear emulsions (Ilford L.4 and Kodak NTA) were exposed by the PuBe source, in a wooden room, 4m × 5m × 3m high, in and around the human phantom, details of which are shown in Figs. 1 and 2. Tracks in the developed emulsions were scanned and analyzed.

Neutron source

LRL source PuBe #593 was used. It is a cylinder, 1.30 in. o.d. × 3.69 in. high, containing 80 g of plutonium. The total emission rate was 5.89×10^6 n/sec.

Nuclear emulsions

Ilford L.4 600-micron emulsions were cut into four pieces (25 × 19 mm or 1 × 3/4 in.) from an original piece (1 × 3 in.), and each was wrapped with black paper and black tape. Each emulsion was sealed in a 20-mil polyvinyl packet with Kodak NTA type film. Each packet was so oriented that the emulsions were exposed normal to the source, which was 50 cm from the center of the phantom.

Phantom

The human phantom was a right elliptical cylinder, 20 × 36 cm by 60 cm high made of 0.65-cm polyethylene (Figs. 1 and 2) and filled with tissue-equivalent fluid.* It stood on a support 76 cm above the floor. Six polyvinyl

---

* Tissue-equivalent fluid:

H_2O,	75 lb;
urea,	9.46 lb;
sucrose,	24.7 lb;
cresol,	1.05 lb.

packets of films (C-1 through C-5, and C-9) were kept during the exposure on the mid-horizontal plane of the phantom with a thin plastic plate. Figure 2 shows the locations of these packets.

Developing and fixing

After the exposure of 87 hours and 20 minutes, the L.4 films were opened in a darkroom and were measured for thickness and lateral extent. They were then developed and fixed by a modified cold-cycle process* in which the solutions were kept at 5°C. To reduce thickness shrinkage, the processed emulsions were soaked in a concentrated solution of wood rosin in ethanol (35 g per 100 ml) for 24 hr. Emulsion history charts (Fig. 3) were kept for each film. The thickness and lateral extent of the processed films were remeasured and the shrinkage factors f_1 and f_2 were calculated for each emulsion. Prior to scanning, films were mounted on 1 × 3 in. microslides with clear epoxy cement.

The NTA films were developed according to the usual method.

---

* A modified cold-cycle process:

45 min	water	(presoak)
90 min	developer:	Na_2SO_3, 3.6 g; $Na_2S_2O_5$, 0.5 g; 10% KBr solution, 4.4 ml; Amidol, 1.6 g; H_2O, 500 ml
45 min	stop bath:	HAc, 1 ml; H_2O, 500 ml
18 hr	fix:	$Na_2S_2O_3$, 150 g; $Na_2S_2O_5$, 11.2 g; H_2O, 500 ml
4 hr	water	(dilution and washing)
3 hr	EtOH	(to dry): gradual dilution to 100% EtOH
24 hr	rosin	(soak)
2 hr	air	(to dry between silk)

Scanning

The Ilford films were scanned by use of the three-axis digitized microscope and apparatus in Figs. 4 and 5. The date, the relative humidity at the time of scanning, the emulsion number, and the end-point coordinates of two tracks were recorded on each punched card. The microscope was fitted with a 65× oil-immersion objective and 10× wide-field eyepieces. It required 5 hr to scan 900 tracks.

The emulsions were exposed so that each contained 10^5 to 10^6 proton tracks. We obtained a 900-track sample from each by taking a microscopic "random walk" through an emulsion, seeking out the track ending nearest to the end point of the previous track. This technique allows rapid scanning, but introduces a sampling bias against short tracks; a correction for this bias is made later, however. Only tracks that had both end points within the emulsion were recorded; i.e., the hydrogen in the emulsion served as an internal radiator, and was the sole source of accepted proton recoils.

Analysis of tracks in nuclear emulsions

The punched cards were analyzed by an IBM-650 Computer with a special computer program called "RECOIL I." This program is designed to calculate the proton recoil energy spectrum in nuclear emulsion exposed to neutrons. The following conditions apply to "RECOIL I."

a. The emulsion must be of 625 microns nominal initial thickness.
b. The emulsion must be of "standard" composition, i.e., density ≈ 3.8 at 50% relative humidity and 20°C.
c. The input tracks scanned must be a random sample of the tracks present in the emulsion, or a suitable correction must be made.
d. The exposure must be roughly isotropic.

The input to RECOIL I consists of rectangular coordinates $(x_1\ y_1\ z_1,\ x_2\ y_2\ z_2)$ for the beginning and end points of a track measured in the emulsion. For each track a correct length in microns is computed,

$$\ell = (f_1^2\,\Delta x^2 + f_1^2\,\Delta y^2 + f_2^2\,\Delta z^2)^{\frac{1}{2}}$$

where ℓ is the length of the track, f_1 is the correction factor for the lateral (x,y) shrinkage, and f_2 is a correction containing the thickness (z) shrinkage factor. The Δx -- i.e., $(x_1 - x_2)$ -- and Δy -- i.e., $(y_1 - y_2)$ -- are in units of microns, but Δz is in units of 0.60 micron. Therefore the correction f_2 is the product of 0.60 × the z shrinkage factor. The program compares the computed length with a range-energy table for protons in nuclear emulsion (Fig. 6), and the track is sorted into one of 85 energy intervals. Several hundred tracks thus generate the points of a raw proton-recoil energy spectrum.

RECOIL I corrects the raw proton spectrum by a function based on geometry. This function gives the probability that a track of a given length which originates in the emulsion will end in the emulsion. Using 625 μ for the emulsion thickness at exposure, and assuming an infinite lateral extent for the emulsion (although the actual size is as small as a 2.0-cm square), we find this function for isotropic exposure is

$$P = \frac{625 - 0.5\ell}{625} \quad \text{for } \ell < 625 \text{ microns,}$$

and

$$P = \frac{312}{\ell} \quad \text{for } \ell > 625 \text{ microns.}$$

These equations are derived in the Appendix, as well as those for "face-normal" exposure. The exposure of the experimental emulsions in and around the phantom was somewhere between the face-normal and isotropic

cases; but since Fig. 7 reveals that the correction is very nearly the same, we used the isotropic correction.

Each point on the spectrum is also corrected by its energy interval. RECOIL I thus computes 85 proton-recoil spectrum points $\frac{\Delta N}{P\Delta E}$ and the standard deviation $\frac{\sqrt{\Delta N}}{P\Delta E}$ for each point, where ΔN is the number of tracks in energy interval ΔE and P is the geometry correction. In addition, the track density in the L.4 films was independently measured by counting the number of tracks (in depth) from 6 to 28 fields of view. The volume per field was 3.34×10^{-5} cm^3.

The number of tracks in depth per field of view for NTA was measured by the standard method. The field was 0.00060 cm^2 when 450× magnification was used.

III. RESULTS

The proton-recoil energy spectra in and around the human phantom, as computed from tracks scanned in Ilford L.4 emulsions C-1 through C-5 and C-9, are given in Table I. The values shown are $\frac{\Delta N}{P\Delta E}$ normalized to give $\Sigma \frac{\Delta N}{P\Delta E} = 10{,}000$. The normalization allows direct comparison of the spectra, channel by channel. These values, converted to give the absolute differential proton track spectra found in the emulsions, are plotted in Figs. 8 through 12. Superimposed on each plot is the proton recoil energy spectrum of the 80-g PuBe source as recorded in emulsions C-9 and C-14 exposed in air at 50 cm. The neutron spectrum to which the phantom was exposed is given in Fig. 13 and is based on analysis of 10,000 tracks in emulsion C-14. In each case the actual data points are given, but the line through the points has been corrected for the sampling bias by the empirically determined factor

$$f = 0.44\ E^{-2.3},\ \text{where}\ E = 0.4\ \text{to}\ 0.66\ \text{MeV}.$$

There is no sampling correction for tracks of energy greater than 0.66 MeV, and it is assumed that the proton spectra are constant below 0.4 MeV. The sampling-correction factor is based on analysis of proton recoil spectra obtained from emulsions exposed to monoenergetic neutrons of energy 0.5 to 5 MeV. The assumption that the proton spectra are constant below 0.4 MeV seems justified by the extensive measurements by de Pangher on the PuBe neutron spectrum,[2] which rule out a large number of low-energy neutrons.

Table 2 lists the proton track data obtained from the Ilford emulsions. These include the air-equivalent neutron exposure at the point of interest in the phantom, and the % of the tracks lost in the region 0 to 0.66 MeV by sampling inefficiency and bias. The measured track densities are corrected for this to yield the corrected track density per unit exposure, average proton energy with and without the n,p track component, and percent n,p tracks. From this the listed dose information is obtained.

The Kodak NTA response to the neutron irradiation at various depths in the phantom is presented in Fig. 14, which also contains for comparison the relative Ilford emulsion response.

Average energy and absorbed dose of proton recoils in the emulsions at various depths in the phantom were found as follows. To obtain the average energy of the proton recoils (Fig. 15) we calculated $\Sigma \frac{\Delta N}{P \Delta E} \cdot E \, \Delta E / \Sigma \frac{\Delta N}{P \Delta E} \cdot \Delta E$ for the Ilford films C-1 to C-5, and C-9. The energy absorbed in the emulsion from proton recoils at various phantom depths is the product of the measured absolute track density and the average energy per track.

IV. DISCUSSION

The estimate of biological damage from ionizing radiation is usually based on the knowledge of the amount of energy imparted to the tissue and by what means, and on the energy distribution of the particles involved. The major part of the dose delivered by fast neutrons to tissue arises from hydrogen nuclei recoiling from elastic collision with the neutrons. In order to understand the biological effects of neutrons in humans it is necessary to know the detailed proton-recoil energy distribution at various depths within the body. Therefore, a suitable tissue neutron dosimeter is one that does not influence the local neutron distribution. Further, it must record exactly the recoil events in space, and it must be of small size. It is also desirable that the dosimeter be continuously sensitive, that it have a low gamma sensitivity, that many simultaneous measurements can be made, that the time between exposure and analysis be convenient, and that a permanent record be made. It is clear that nuclear track emulsion is superior to other dosimeters in these respects.

Used as described in this paper, nuclear emulsion is an absolute fast-neutron dosimeter which also yields the local differential proton tissue dose. Neutron-dose information can also be obtained by measurements with various metal foils, scintillators, and gas-filled proportional counters. The major advantage of all these detectors is the rapid availability of their information during or immediately following the irradiation, whereas 600-μ emulsion requires several days for development and scanning before yielding the dose information. The major disadvantages of scintillators and proportional counters are their size, and their dependence on attached electronic apparatus. The latter makes them considerably less versatile than foils and emulsion; and their size without question alters the local fast-neutron distribution and

makes it difficult to take measurements inside a human-sized phantom. Metal foils are basically neutron flux meters, and obtaining precise dose information from foils is difficult, even when they have been calibrated by the very neutron source whose tissue dose is being measured.

Table 3 gives the basic data concerning the effect of the presence of track emulsion on the local neutron distribution in tissue. The table reveals that for fast neutrons the total macroscopic cross sections of tissue and emulsion are nearly the same. Therefore the presence of emulsion is not expected to perturb the local fast-neutron spectra at various depths in tissue.

When fast neutrons impinge on the human body, large numbers of thermal neutrons are produced as the fast neutrons lose energy through multiple collisions. This is why the effect of a dosimeter on the local thermal-neutron density must also be considered. The ratio of the macroscopic absorption cross section for thermal neutrons in emulsion and in tissue is about 30/1. However, this does not appear to be important when the mean-square diffusion distance (as the crow flies) of thermal neutrons is compared to the emulsion thickness. This "distance" is about 16 cm^2 in tissue and 1 cm^2 in emulsion; the emulsion thickness is 0.060 cm. This means that the average net distance that a neutron travels from the time when it is produced until the time when it is captured is about 1 cm in emulsion and 4 cm in tissue. Therefore the thermal neutron density in the emulsion is not expected to differ from that in nearby tissue.

1. Interpretation of the track density distributions

The major feature of these track spectra, as revealed in Figs. 8 - 12, is that from about 0.8 to 2.5 MeV the track density decreases exponentially,

being proportional to $e^{-0.7E}$. Beyond 3 MeV, it is proportional to $e^{-0.9E}$. This track-density distribution is what one theoretically expects for a PuBe neutron exposure of emulsion in air*. Proton recoil tracks from the thermal $N^{14}(n, p)C^{14}$ reaction, and from secondary neutron collisions with hydrogen nuclei, are superimposed on the basic distribution. The n, p tracks are monoenergetic at 0.60 MeV and are quite prominent in the track spectra of emulsions C-2, C-3, and C-4. The secondary-collision tracks are largely below 1.5 MeV and are evident in the track spectra C-1 to C-4. The track density spectrum of C-5 shows the basic pattern with a relatively small thermal-neutron $N^{14}(n, p)C^{14}$ peak and only a slight secondary-neutron collision shift. The finding that the same distribution obtains at various depths indicates that the major features of the neutron spectrum are present even deep in the phantom.

Below 0.5 MeV, the efficiency of nuclear emulsion drops rapidly, giving the erroneous picture that the number of tracks falls. The track densities are expected to be about the same from 0.5 to 0 MeV as they are at 0.5 MeV. The curves have been corrected for this and for sampling bias, as discussed in the previous section.

2. Separation of the thermal $N^{14}(n, p)C^{14}$ track component, and estimation of the thermal neutron intensities

For determining proton-recoil emulsion dose there is no need to separate the component due to n, p tracks, but it is important that this be done for calculating tissue dose.

---

*The expected track-density distribution was calculated from unpublished data on the PuBe neutron spectrum obtained by Lehman.

The thermal n,p track contribution was estimated by subtracting the percent of the tracks in the 0.54- to -0.66-MeV interval of the C-9 distribution (in which we assume there are no n,p tracks) from the percent in the same region in emulsions C-1 through C-5:

$$\text{percent of thermal-neutron n,p tracks} = A_i - (1 - A_i)\, k, \tag{1}$$

where A_i is the percent of tracks in the 0.54- to -0.66-MeV region for the emulsion under consideration and k is $A/(1 - A)$ for emulsion C-9. Table 4 gives the result.

3. Interpretation of total L.4 track density and total NTA response vs depth in phantom

The major feature of the plots in Fig. 14 is the exponential attenuation of neutrons with depth, with an attenuation half thickness of 7.0 cm. This attenuation is for all fast neutrons present in the phantom that are detectable by nuclear track emulsion. Superimposed on this basic response is the response due to thermal-neutron $N^{14}(n,p)C^{14}$ tracks. It is this thermal-neutron response that distorts the basic 7.0 cm attenuation in the L.4 plot, causing the extended hump in the center of the curve. The following brief explanation is an attempt to clarify this.

The NTA response to neutron exposure, in tracks/field, may be represented by the equation

$$\text{NTA response} = an^{th} + bn^{f}. \tag{2}$$

Similarly, the L.4 response, in tracks/cm^3, may be represented by

$$\text{L.4 response} = cn^{th} + dn^{f}. \tag{3}$$

In these equations, the coefficients a and b have the dimensions of tracks/field per unit thermal neutron (n^{th}) or fast neutron (n^{f}) per cm^2.

The thermal n, p track contribution was estimated by subtracting the percent of the tracks in the 0.54- to -.66-Mev interval of the C-9 distribution (in which we assume there are no n, p tracks) from the percent in the same region in emulsions C-1 through C-5:

percent of thermal-neutron n, p tracks =

$$A_i - (1-A_i)k, \tag{1}$$

where A_i is the percent of tracks in the 0.54- to -0.66-Mev region for the emulsion under consideration and k is A/(1-A) for emulsion C-9. Table 4 gives the result.

3. Interpretation of total L.4 track density and total NTA response vs depth in phantom

The major feature of the plots in Fig. 14 is the exponential attenuation of neutrons with depth, with an attenuation half thickness of 7.0 cm. This attenuation is for all fast neutrons present in the phantom that are detectable by nuclear track emulsion. Superimposed on this basic response is the response due to thermal-neutron $N^{14}(n,p)C^{14}$ tracks. It is this thermal-neutron response that distorts the basic 7.0 cm attenuation in the L.4 plot, causing the extended hump in the center of the curve. The following brief explanation is an attempt to clarify this.

The NTA response to neutron exposure, in tracks/field, may be represented by the equation

$$\text{NTA response} = an^{th} + bn^{f}. \tag{2}$$

Similarly, the L.4 response, in tracks/cm^3, may be represented by

$$\text{L.4 response} = cn^{th} + dn^{f}. \tag{3}$$

In these equations, the coefficients a and b have the dimensions of tracks/field per unit thermal neutron (n^{th}) or fast neutron (n^{f}) per cm^2.

The coefficients c and d have the dimensions tracks/cm^3 per unit thermal- or fast-neutron exposure. The difference in shape between the curves in Fig. 14 arises because $c/d \approx 3\ a/b$ for PuBe neutrons, that is, the relative response of L. 4 to thermal neutrons, is roughly three times that of NTA. The reason that these ratios differ is that the NTA response includes tracks which originate in adjacent hydrogenous radiator material,[3] whereas the L. 4 response does not. (Only tracks that begin and end within the L. 4 emulsion are scanned.)

4. Calculation of tissue dose vs depth in the phantom

To obtain the tissue thermal-neutron n, p track dose, the L. 4 dose is multiplied by 0.406, the ratio of the nitrogen atomic density in tissue to that in L. 4 emulsion. The result is plotted in Fig. 17 where the n, p tissue dose calculated here is shown to agree with the relative thermal neutron density measured by indium foil activation. To obtain the fast neutron proton track dose, the L. 4 dose is multiplied by 1.86, the ratio of the atomic density of hydrogen in tissue to that in L. 4 emulsion.

Fig. 16 gives the absolute differential proton tissue dose in tissue-equivalent liquid at various depths in the phantom. These curves were obtained from the basic track data in Table 1 by computing the points $\left(E \cdot \frac{\Delta N}{P \Delta E}\right)_i$. Then the area under the n, p track peak at 0.60 MeV was reduced by 4.6, the factor giving the relative n, p response in emulsion as compared with tissue, and the points below 0.66 MeV were corrected as described earlier. The plotted curves are the smooth lines through the calculated points $\frac{E \cdot \Delta N}{P \Delta E}$. The curves are normalized so that the total area under each curve equals the total dose, obtained from the product of the track density in tissue by the average proton energy in tissue. The error (in %) at any given energy on

these curves is roughly that of the proton track spectra at the same energy given in Table 1.

The differential dose values listed in Table 5 were obtained by finding the fractional areas under the dose curves in Fig. 16. It should be stressed that the dose distributions obtained here are the averages for about 200 millirad total exposure. Shorter exposures give track-by-track quantum distributions which approximate those shown here only if the exposures are roughly as great as those used in this work.

5. Comparison of phantom proton dose with a predicted dose

In Handbook 63[4] the tissue proton dose is calculated by assuming exposure of an infinite 30-cm-thick tissue-equivalent slab to monoenergetic neutrons of various energies. Table 6 compares the data for 2.5- and 5.0-MeV neutrons with our phantom data for PuBe neutrons. Two things are evident — the first is that at all depths our values are roughly 2/3 the 5.0-MeV values in Handbook 63. The second is that the proton dose attenuation with depth shows a half-thickness value of 10 cm for the phantom exposed to PuBe neutrons, compared with 5.5 cm and 8.5 cm for the slab exposed to 2.5- and 5.0-MeV neutrons.

A large part of the discrepancy between our values and the values of Handbook 63 for the absolute magnitude of the proton dose lies in the fact that Handbook 63 uses a value of 2.50 MeV for the average first-collision energy transfer between a 5.0-MeV neutron and a hydrogen nucleus. We found that the average energy of the recoil tracks in the C-1 to C-5 spectra (excluding thermal n, p tracks) varied between 1.21 and 1.57 MeV at the different depths, compared with 1.60 MeV in emulsion C-9, which was exposed

in air. The values at the 0-cm, 5-cm, 10-cm, and 15-cm depths are much lower than 1.60 MeV; this is evidence for a significant track contribution from second-collision neutrons. The average proton track energy at the back surface of the phantom (C-5) is 1.57 MeV – a surprisingly low value, since very few tracks here arise from secondary-neutron collision. This reveals that although there may be some hardening of primary neutron spectrum, many low-energy neutrons are present.

V. SUMMARY

Nuclear track emulsion was evaluated as a neutron dosimeter in the exposure of a human phantom to neutrons from a plutonium-beryllium source. Emulsion pieces were located at various positions in and around the phantom. The following basic information referring to each location was obtained by scanning 2-cm squares of 600-μ Ilford L.4 emulsion with a semiautomatic three-axis digitized microscope:

1. The absolute differential proton-recoil energy spectrum.
2. The average track energy.

From these data, the following dose information may be calculated:

1. The absolute differential local absorbed dose from proton tracks in tissue.
2. The local thermal neutron $N^{14}(n, p)C^{14}$ dose in tissue.
3. The thermal neutron density and fast neutron flux in tissue.

In addition, the proton recoil spectrum reveals general information about the local fast-neutron energy spectrum.

In this experiment the total proton dose to tissue in the phantom varied from 3.1×10^{-9} rad at the front surface to a low of 0.63×10^{-9} rad at the

back surface per unit exposure to PuBe neutrons. Although large numbers of $N^{14}(n, p)C^{14}$ tracks were observed inside the phantom, their contribution to the total dose in no case exceeded 2%.

Acknowledgments

The authors wish to thank Mr. James C. Hodges for the design, construction, and maintenance of the three-axis digitized microscope; Mr. Arthur W. Barnes for the design of the microscope electronics; Mr. John R. Meneghetti for making the phantom; Mr. John H. Wood and Miss Betty J. Lofstrand for processing the L.4 emulsions; Miss Olga M. Fekula for scanning the L.4 emulsions; Miss Dorothy A. Hadley and Miss Josephine A. Camp for scanning the NTA film; Mr. Carl Quong for preparing the computer program; and Mr. H. Wade Patterson and Dr. Roger W. Wallace for their continuous support.

Footnotes and References

*Work done under the auspices of the U. S. Atomic Energy Commission.

1. W. H. Barkas, et al., The Range-Energy Relation in Emulsion, Part II, University of California, Lawrence Radiation Laboratory Report UCRL-3769, April 15, 1957 (unpublished).
2. J. de Pangher, A Reproducible Precision Polyethylene Long Counter for Measuring Fast Neutron Flux (presented at Washington meeting of Am. Phys. Soc., April 24-27, 1961).
3. R. L. Lehman, "Energy Response and Physical Properties of NTA Personnel Neutron Dosimeter Nuclear Track Film," Lawrence Radiation Laboratory Report UCRL-9513, Jan. 13, 1961 (unpublished).
4. Handbook 63, "Protection Against Neutron Radiation up to 30 Million Electron Volts," U. S. Dept. of Commerce, National Bureau of Standards, Nov. 22, 1957.

APPENDIX

(Richard L. Lehman)

The Probability that a Track of Given Length that Originates in the Emulsion Will Also End in the Emulsion

Two cases are considered; face-normal exposure and isotropic exposure. In both cases it is convenient to first consider the situation when the track length ℓ exceeds the emulsion thickness T, as in Fig. 18. Assume the emulsion has infinite lateral extent, and that the probability of a neutron-proton collision does not vary within the emulsion. Consider a track of length ℓ originating at an arbitrary depth T - x in the emulsion. There is cylindrical symmetry about a line normal to the emulsion surfaces through the track origin.

Case 1. Face-Normal Exposure

Only tracks of this length that enter the solid angle about conical angle ϕ end in the emulsion. In this case, the probability that a track will enter any solid angle is not constant, but is given by

$$\frac{dn}{d\Omega} = \frac{N_0}{2\pi}\,\frac{\Omega}{\pi}\,, \tag{1}$$

where $\Omega = 2\pi \sin\phi$. Therefore

$$dP = \frac{dn}{N_0} = \frac{d\Omega}{2\pi}\left(\frac{\Omega}{\pi}\right) \tag{2}$$

(where the quantity in parenthesis may be considered a weighting function);

$$P(x) = \int_0^{\frac{2\pi x}{\ell}} \frac{\Omega}{2\pi^2}\, d\Omega = \frac{x^2}{\ell^2}\,; \tag{3}$$

and

$$P = \int_0^T \frac{x^2}{\ell^2}\,\frac{dx}{T} = \frac{T^2}{3\ell^2}\,. \tag{4}$$

To obtain P for $\ell < T$, one divides the thickness of the emulsion into two pieces, ℓ and $T-\ell$.

For the fraction $\frac{\ell}{T}$ the probability is $\frac{1}{3}$, as given by Eq. (4), where ℓ = "T". For the fraction $\frac{T-\ell}{T}$ the probability is unity. Therefore

$$P(\ell < T) = \frac{\ell}{3T} + \frac{T-\ell}{T} = 1 - \frac{2\ell}{3T}. \tag{5}$$

Case 2. Isotropic Exposure

Only tracks of this length that enter the solid angle of cone ϕ end in the emulsion. In this case,

$$\frac{dn}{d\Omega} = \frac{N_0}{4\pi} = \text{constant}, \tag{6}$$

and

$$dP = \frac{dn}{N_0} = \frac{d\Omega}{4\pi} \quad (1) \tag{7}$$

(the quantity in parenthesis is a weighting function, corresponding to that in Case 1),

$$P = \int_0^{\frac{2\pi x}{\ell}} \frac{d\Omega}{4\pi} + \int_0^{2\pi \frac{T-x}{\ell}} \frac{d\Omega}{4\pi}, \tag{8}$$

where

$$\frac{x}{\ell} = \cos(\phi' - \theta) \text{ and } \frac{(T-x)}{\ell} = \cos\theta, \tag{9}$$

$$P = \frac{x}{2\ell} + \frac{T-x}{2\ell} = \frac{T}{2\ell} \text{ independent of } x. \tag{10}$$

As in Case 1, to obtain $P(\ell < T)$, the probability for the fraction $\frac{\ell}{T}$ is $\frac{1}{2}$, and that for the fraction $\frac{T-\ell}{T}$ is unity. Therefore

$$P(\ell < T) = \frac{\ell}{2T} + \frac{T-\ell}{T} = 1 - \frac{\ell}{2T}. \tag{11}$$

Table 1. Energy spectrum of proton recoils in emulsions.

Channel	Energy (Kev)	C-1	S.D.	C-2	S.D.	C-3	S.D.	C-4	S.D.	C-5	S.D.	C-9	S.D.
1	30	..	..	..	..	..	..	..	..	..	..	..	..
2	120	..	..	8	8	..	..	..	..	..	..	..	..
3	224	..	..	10	10	10	10	..	..	11	11	11	11
4	315	87	33	45	22	59	26	20	14	26	18	29	18
5	396	390	74	151	44	238	56	165	43	87	36	180	50
6	468	273	64	383	72	273	63	240	54	237	61	287	66
7	535	506	91	575	92	434	82	453	77	136	48	325	73
8	600	726	112	1155	134	1049	131	904	111	595	104	517	94
9	665	397	85	1173	138	1215	144	1244	133	697	115	342	78
10	722	604	107	1158	140	1378	157	1106	129	650	113	677	113
11	777	582	106	754	115	700	114	739	107	608	111	561	104
12	857	454	68	474	66	517	70	560	67	580	78	574	76
13	959	499	73	431	64	403	64	387	57	510	75	381	64
14	1057	468	72	362	60	296	56	291	51	395	68	355	63
15	1149	416	69	365	62	318	59	320	54	458	74	460	73
16	1232	400	70	318	59	276	56	250	49	507	80	375	67
17	1320	479	78	296	58	215	51	390	62	395	72	541	82
18	1403	498	81	213	50	261	57	291	55	479	81	327	65
19	1484	433	77	293	60	244	56	268	54	240	58	297	63
20	1560	366	72	204	51	201	52	257	54	324	69	379	73
21	1635	321	68	132	42	166	48	173	45	274	65	349	71
22	1719	291	54	172	40	257	50	263	46	294	56	310	56
23	1825	199	46	171	40	179	42	175	38	296	57	293	55
24	1919	221	43	141	32	109	29	169	33	274	48	245	45
25	2050	235	45	181	38	239	44	145	32	191	42	260	47
26	2189	183	37	119	28	125	29	145	29	214	40	160	34
27	2330	182	37	103	27	101	27	192	34	182	38	181	37
28	2500	127	26	70	19	110	24	118	23	150	29	198	33
29	2700	100	23	62	17	75	19	75	18	110	25	194	32
30	2909	85	22	87	21	43	15	63	17	142	29	147	29
31	3100	94	24	64	18	89	22	84	20	166	32	164	31
32	3300	65	19	49	15	77	20	73	18	84	22	172	30
33	3500	62	19	46	15	27	12	62	17	112	26	106	24
34	3700	48	17	22	11	34	14	43	14	82	23	126	28
35	3890	34	14	31	13	60	18	50	15	72	21	34	14
36	4090	42	16	32	13	51	17	52	16	87	23	60	19
37	4294	11	8	30	12	26	12	26	11	46	16	66	19
38	4489	6	6	10	7	27	12	41	14	48	17	51	17
39	4690	18	11	22	11	..	..	39	14	19	11	31	14
40	4900	17	10	5	5	5	5	23	10	54	18	57	18
41	5110	30	13	11	8	11	8	5	5	25	12	29	13
42	5310	..	..	11	8	..	..	15	9	26	13	44	17
43	5500	13	9	..	..	6	6	10	7	20	12	7	7
44	5689	13	9	6	6	13	9	5	5	7	7	13	9
45	5880	6	6	23	12	6	6	..	..	7	7	6	6
46	6079	13	9	6	6	..	..	..	..	7	7	13	9
47	6280	..	..	6	6	6	6	15	9	13	9	..	..
48	6489	6	6	..	..	..	..	..	..	20	12	13	9
49	6790	..	..	3	3	..	..	3	3	4	4	7	5
50	7190	..	..	3	3	3	3	3	3	..	..	7	5
51	7600	..	..	..	..	..	..	..	..	4	4	4	4
52	8000	..	..	..	..	4	4	..	..	8	6	4	4
53	8400	..	..	..	..	..	..	..	..	4	4	..	..
54	8800	..	..	4	4	4	4	..	..	..	..	..	..
55	9200	..	..	..	..	4	4	..	..	..	..	..	..
56	9600	..	..	4	4	..	..	7	5	..	..	..	..
57	10000	..	..	4	4	14	8	..	..	5	5	5	5
58	10400	..	..	..	..	42	14	16	8	..	..	15	9
59	10800	..	..	..	..	..	..	..	..	6	6	..	..
60	11200	..	..	..	..	..	..	..	..	12	9	..	..

Table 2. Proton track data from Ilford emulsions exposed to PuBe neutrons.

	Emulsion					
	C-1	C-2	C-3	C-4	C-5	C-9
Air-equivalent neutron exposure (n cm^{-2} $\times 10^{-7}$)	9.5	7.3	5.9	4.9	4.0	5.9
Measured track density (tracks $cm^{-3} \times 10^{-6}$)	6.0	3.65	2.1	1.05	0.43	2.85
Tracks lost 0-0.66 Mev (%)	31	31	31	27	26	24
Correct track density (tracks $cm^{-3} \times 10^{-6}$)	7.9	4.8	2.85	1.33	0.54	3.55
Correct density per unit exposure (tracks cm^{-3} per n cm^{-2})	0.083	0.0655	0.0485	0.027	0.0135	0.060
Average proton track energy (Mev)	1.23	1.11	1.17	1.25	1.55	1.60
Average proton track energy excluding thermal n, p tracks (Mev)	1.26	1.21	1.25	1.34	1.57	1.60
Thermal n,p tracks (%)	3	16	13	12	3	0
Emulsion proton dose (ergs cm^{-3} per n $cm^{-2} \times 10^{7}$)	1.6	1.15	0.91	0.54	0.33	1.55
Dose lost due to tracks lost 0-0.66 Mev (%)	9	9	8.5	7	5	4.5
Thermal n,p dose (%)	1.5	10	8	7	1	0

Table 3. Cross sections in emulsion and tissue.

Element	Atomic density ($\times 10^{22}$ cm^{-3})	σ_{abs}^{th} ($\times 10^{-24}$ cm^2)	$\sigma_{total}^{1\ Mev}$ ($\times 10^{-24}$ cm^2)	$\sigma_{total}^{4\ Mev}$ ($\times 10^{-24}$ cm^2)	$N\sigma_{abs}^{th}$ (cm^{-1})	$N\sigma_{total}^{1\ Mev}$ (cm^{-1})	$N\sigma_{total}^{4\ Mev}$ (cm^{-1})
Emulsion							
Ag	1.01	62.	6.6	4.2	0.626	0.066	0.082
Br	1.00	6.6	5.0	3.9	0.067	0.050	0.039
H	3.21	0.33	4.4	1.9	0.011	0.142	0.061
C	1.38	0.0032	2.6	2.0	0.000	0.036	0.028
O	0.95	0.19	4.0	2.0	0.002	0.038	0.019
N	0.32	1.83	2.0	1.8	0.006	0.006	0.006
I	0.0056	6.7	7.0	5.0	0.000	0.000	0.000
					0.710	0.340	0.195
Tissue							
H	6.00[a]				0.0200	0.264	0.114
C	0.91[a]				0.0000	0.024	0.018
O	2.45[a]				0.0000	0.098	0.049
N	0.13[a]				0.0024	0.003	0.002
					0.022	0.390	0.180

[a]Assuming density of tissue is 1.00

Table 4. Estimation of the n, p track component in Ilford films.

	A_i	k	% thermal n, p tracks	% thermal neutrons present[a]
C-9	0.084	0.092	0	0
C-1	0.119		3.8	19
C-2	0.222		15[b]	54
C-3	0.203		13[c]	49
C-4	0.189		11.5	44
C-5	0.113		3.1	17

$$\frac{n^{th}}{n} = \frac{(\%)6.5}{1 + (\%)5.5} \qquad (\%) = \%\ n, p\ \text{tracks}$$

[a] Based on d/c ratio in Eq. (3) of 6.5/1.

[b] 17.5% by direct count on differential track count.

[c] 13.3% by direct count on differential track count.

Table 5. Proton tissue dose from irradiation by PuBe neutrons.

Depth in phantom (cm)	0	5	10	15	20
Total rad dose ($\times 10^9$) per n cm^{-2} exposure	3.1	2.4	1.8	1.1	0.63
Dose (in %) by protons of energy interval (in Mev):					
0 - 0.5	5.7	6	6	5	4
0.5 - 1.0	14	19	19	17	11.5
1.0 - 1.5	18	16.0	14.5	14	14
1.5 - 2.0	15	12.5	13	12.5	13.5
2.0 - 2.5	11	10	11	10.5	11
2.5 - 3.0	8.6	8.5	8.8	9	9.3
3.0 - 3.5	7.0	7.3	7.5	7.8	8.7
3.5 - 4.0	5.5	5.5	6.1	6.8	8.1
4.0 - 5.0	7.6	7.3	7.8	9.4	11.
5.0 - 6.0	4.4	4.1	3.3	4.4	5.1
6.0 - 7.0	1.8	2.3	1.8	2.3	2.3
7.0 - 10.5	1.4	1.5	1.2	1.3	1.7
Av. proton energy (Mev)	1.25	1.18	1.23	1.32	1.57
n, p tracks (%)	0.8	4.0	3.2	3.0	0.5
n, p dose (%)	0.4	2.0	1.6	1.4	0.2

Table 6. Comparison of measured tissue proton dose in phantom with Handbook 63 calculated dose for an infinite 30-cm-thick slab of tissue.

Depth (cm)	Tissue proton dose (rad per $n/cm^2 \times 10^{+9}$)		
	Phantom, PuBe neutrons	HB 63, 2.5-Mev neutrons	HB 63, 5.0-Mev neutrons
0	3.1	3.7	4.8
5	2.4	2.8	4.1
10	1.8	1.4	2.6
15	1.1	0.65	1.7
20	0.63	0.31	1.1

br\

FIGURE CAPTIONS

Fig. 1. Positions of phantom and source.

Fig. 2. Positions of source, phantom, and packets during exposure (as viewed from above).

Fig. 3. Chart used for recording emulsion history.

Fig. 4. Three-axis digitized microscope with supporting electronic equipment.

Fig. 5. Three-axis digitized microscope used in this experiment.

Fig. 6. Range-energy relation for protons in standard nuclear emulsion and in water after Barkas, et al. (Ref. 1).

Fig. 7. Plot of geometric correction factors for isotropic, and for face-normal exposure of 625-μ emulsion.

Fig. 8. Energy distribution of recoil protons from PuBe source: Emulsion C-1, at front surface of phantom.

Fig. 9. Energy distribution of recoil protons from PuBe source: Emulsion C-2, 5.65 cm deep in phantom.

Fig. 10. Energy distribution of recoil protons from PuBe source: Emulsion C-3, 10.65 cm deep in phantom.

Fig. 11. Energy distribution of recoil protons from PuBe source: Emulsion C-4, 15.65 cm deep in phantom.

Fig. 12. Energy distribution of recoil protons from PuBe source: Emulsion C-5, 21 cm deep in phantom (on the back surface).

Fig. 13. An 80-g PuBe neutron source spectrum, obtained from nuclear emulsion.

Fig. 14. Numbers of tracks in Kodak NTA emulsion (30μ) at various depths in the phantom, and the relative track density in L.4 emulsions.

FIGURE CAPTIONS (Continued)

Fig. 15. Average energy of recoil protons in nuclear emulsion at various depths in the phantom. —— experimental data. —— same data with thermal n,p tracks omitted.

Fig. 16. Absolute differential proton tissue dose at various depths in the phantom.

Fig. 17. Tissue dose by protons from thermal-neutron-induced $N^{14}(n,p)C^{14}$ protons in phantom exposed to PuBe neutron source. —— estimated from measurements (this experiment). - - - - thermal-neutron density in phantom, measured by indium foil activation with same exposure conditions (relative numbers only, to allow comparison of curve shapes).

Fig. 18. Cross section of a piece of nuclear emulsion of thickness T.

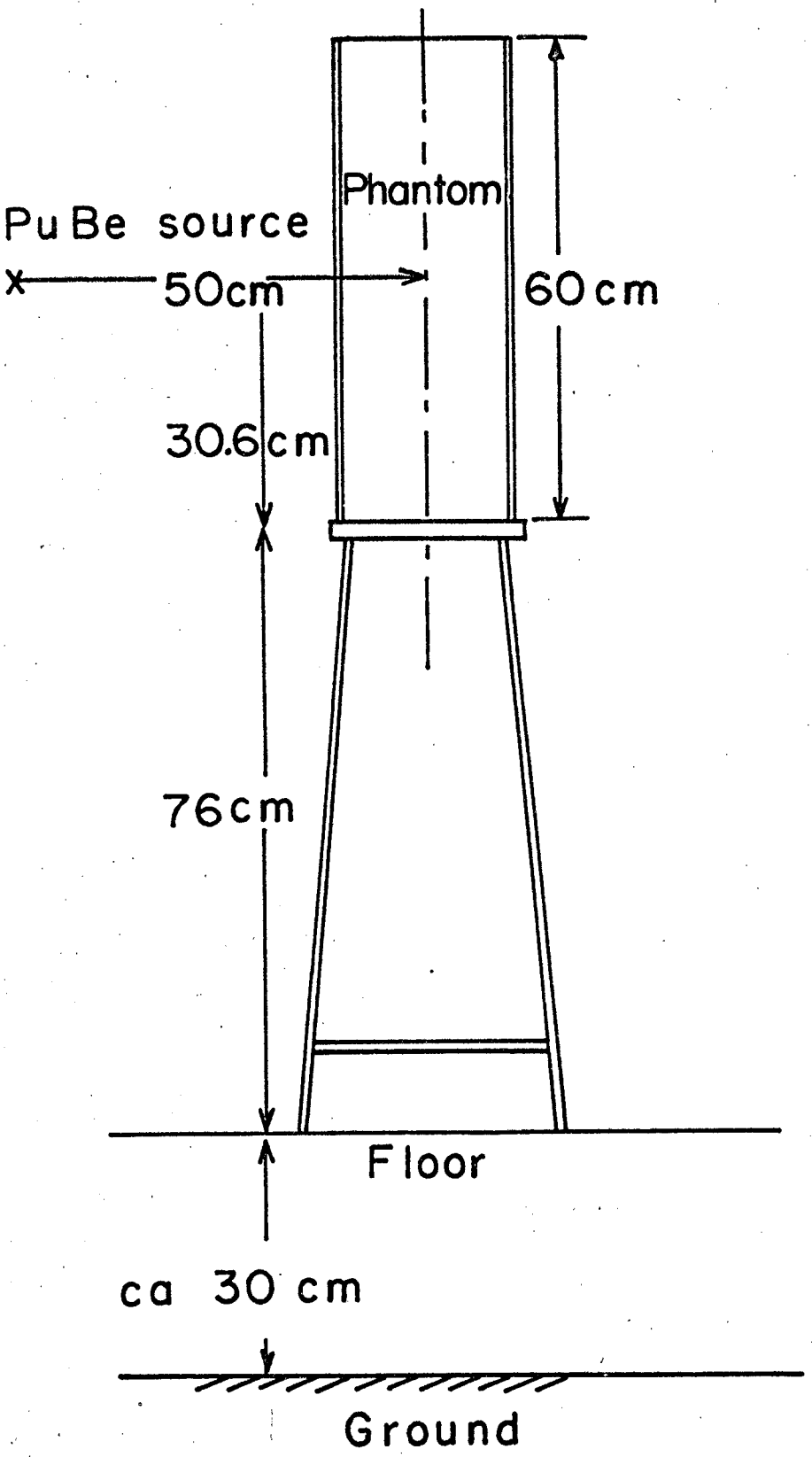

Fig. 1. MU-25269

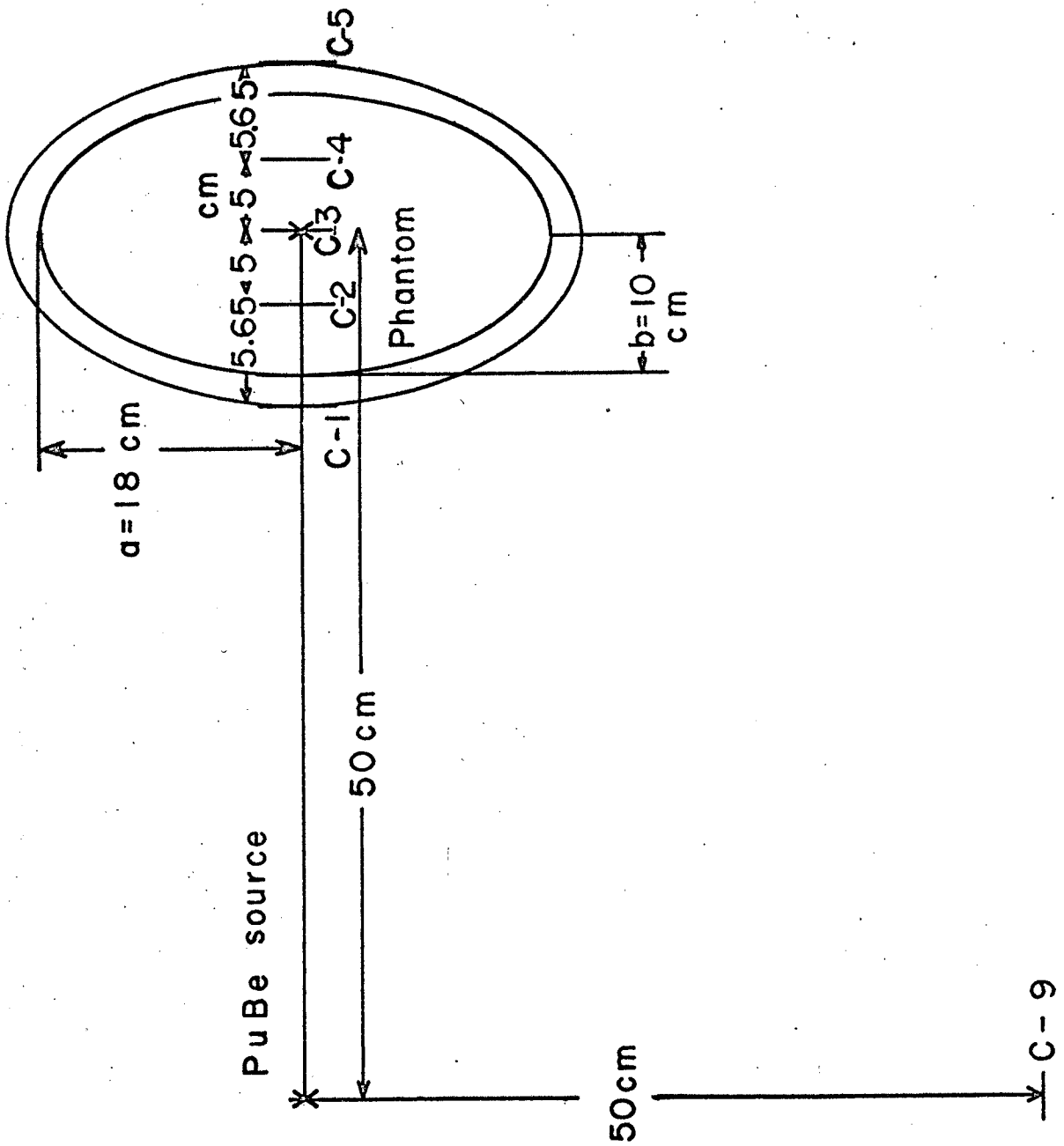

MU-25270

Fig. 2.

EMULSION HISTORY CHART

Emulsion # C-1 Type L.4 IHford 600μ Batch code Z-2581
Date Manufactured 8-9-61 Date of arrival at UCLRL 8-23-61
Storage: Location I House Dates 8-23-61 to 8-29-61
Location Bldg 72 Rm 108 Dates 8-29-61 to 9-1-61
Location Bldg 47 Tech Photo Dates 9-5-61 1100 to 9-7-61 date devel.

Exposure: Location Bldg 80A Type of exposure PuBe neutron source #595
Duration 1640 9-1-61 to 0800 9-5-61 Distance from source 39.4 cm.
Orientation Normal to axis of incident neutrons. Outside front center of
Scattering conditions Phantom containing "tissue equivalent" liquid.
Diagram See Notebook

Development: Procedure Modified cold cycle + 24 hr soak in ethanolic rosin sol'n.
Personnel B. Lofstrand and J. Wood
Location Bldg 47 Tech Photo Dates 9-7-61 to 9-11-61
Comments Well developed throughout.

Mounting: 1 X 3 glass slide ✓ Epoxy cement ✓ Date 9-13-61 Person RLL
Comments Mounted with C-2 and C-3

Scanning: Scanner O.M. FEKULA No. of tracks 438 Dates 9-27-61 to →
Scanner ____ No. of tracks ____ Dates ____ to ____
Location of data cards ____ Emulsion code no. 301 f_1 0.990 f_2 0.660
Comments Easy to scan 5.4×10^6 t/cm³ (avg. of 10 fields in depth)

Analysis: Program RECOIL I Tracks used 438 Date 9-28-61 Person RLL
Program RECOIL IP Tracks used 438 Date 1-23-62 Person RLL
Program ____ Tracks used ____ Date ____ Person ____
Comments No stops - a good computer run 1-23-62.

Shrinkage: Thickness before presoak - micrometer (inches)
Date 9-5-61 RH 50% .0256 .0255 .0253 .0262 .0266 Av 0.0258 in.

C-1

Thickness after development - before mounting - micrometer
Date 9-13-61 RH 60% .0233 .0240 .0232 .0236 .0234 Av 0.0235 in.

Thickness after mounting - microscope
Date ____ RH ____ Average ____ μ X .393 = 0.0 in.

Lateral Distortion: Dimensions before presoak - 64th inch scale
Date 9-5-61 50/64 51/64 64/64 64/64 Av 57.2/64

C-1

Dimensions after development - before mounting
Date 9-13-61 51/64 53/64 66/64 66/64 Av 59/64

Dimensions after mounting
Date ____ ____ ____ ____ ____

Subsequent Measurements: $f_1 = \frac{57.2}{59} = 0.97$ $f_2 = 0.600 \times \frac{258}{235} = 0.66$
Note that the rosin soak treatment reduces the vertical (z) shrinkage to 11% in this case.

Fig. 3.

MU-26968

Fig. 4.

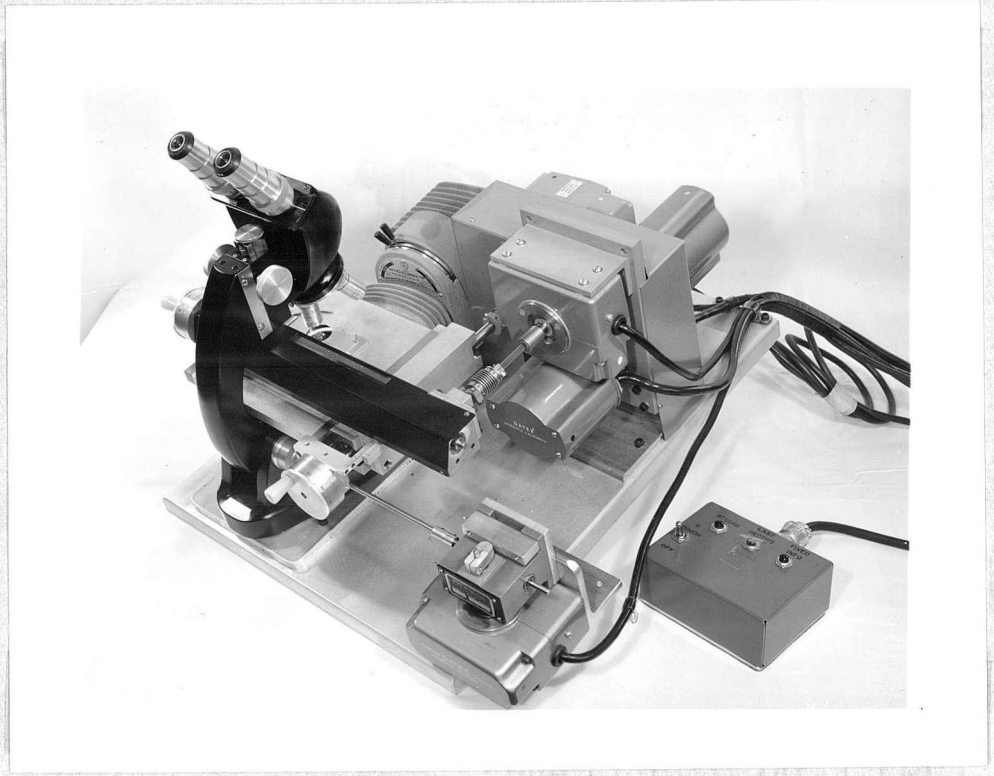

Fig. 5.

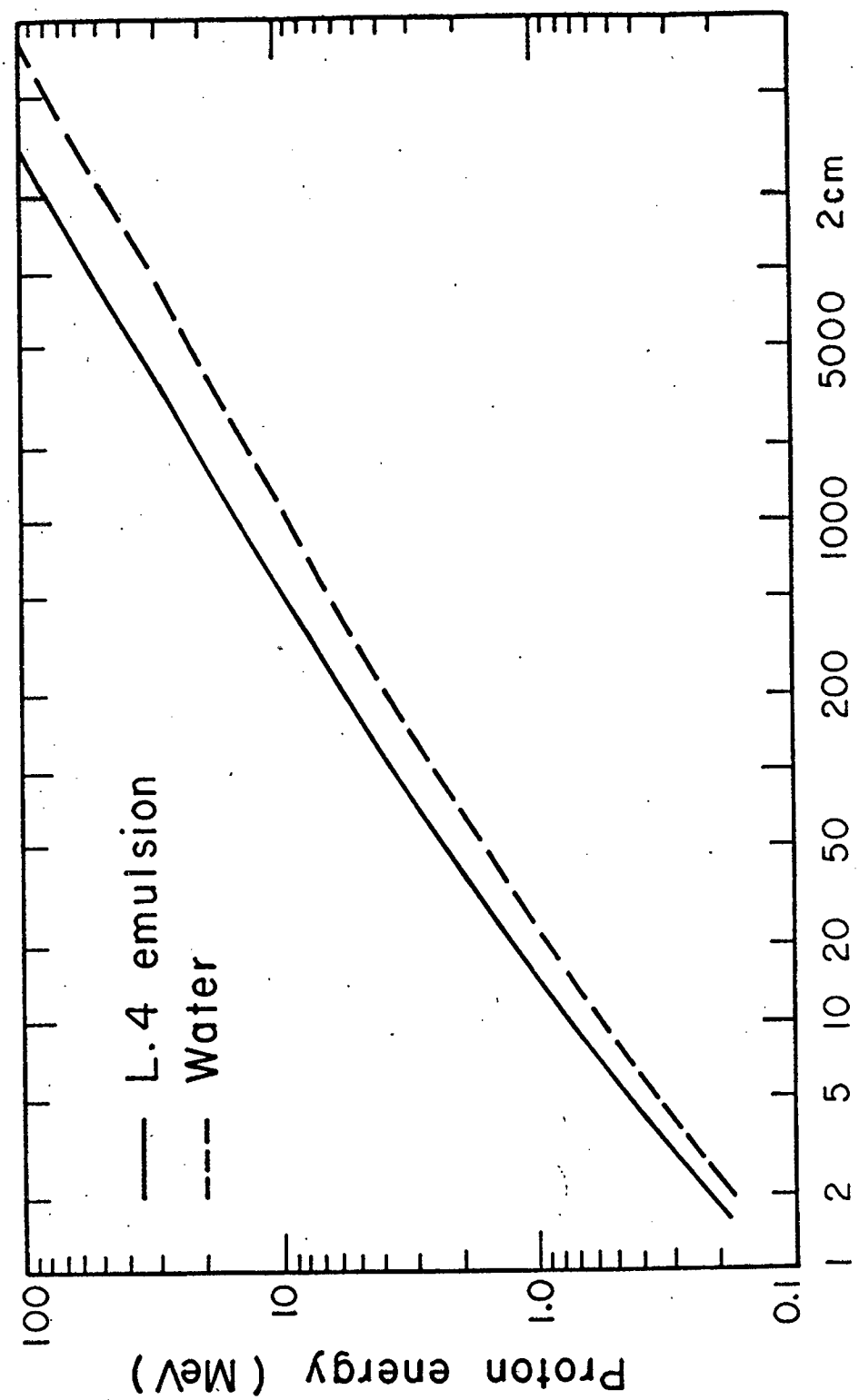

MU-26966

Fig. 6.

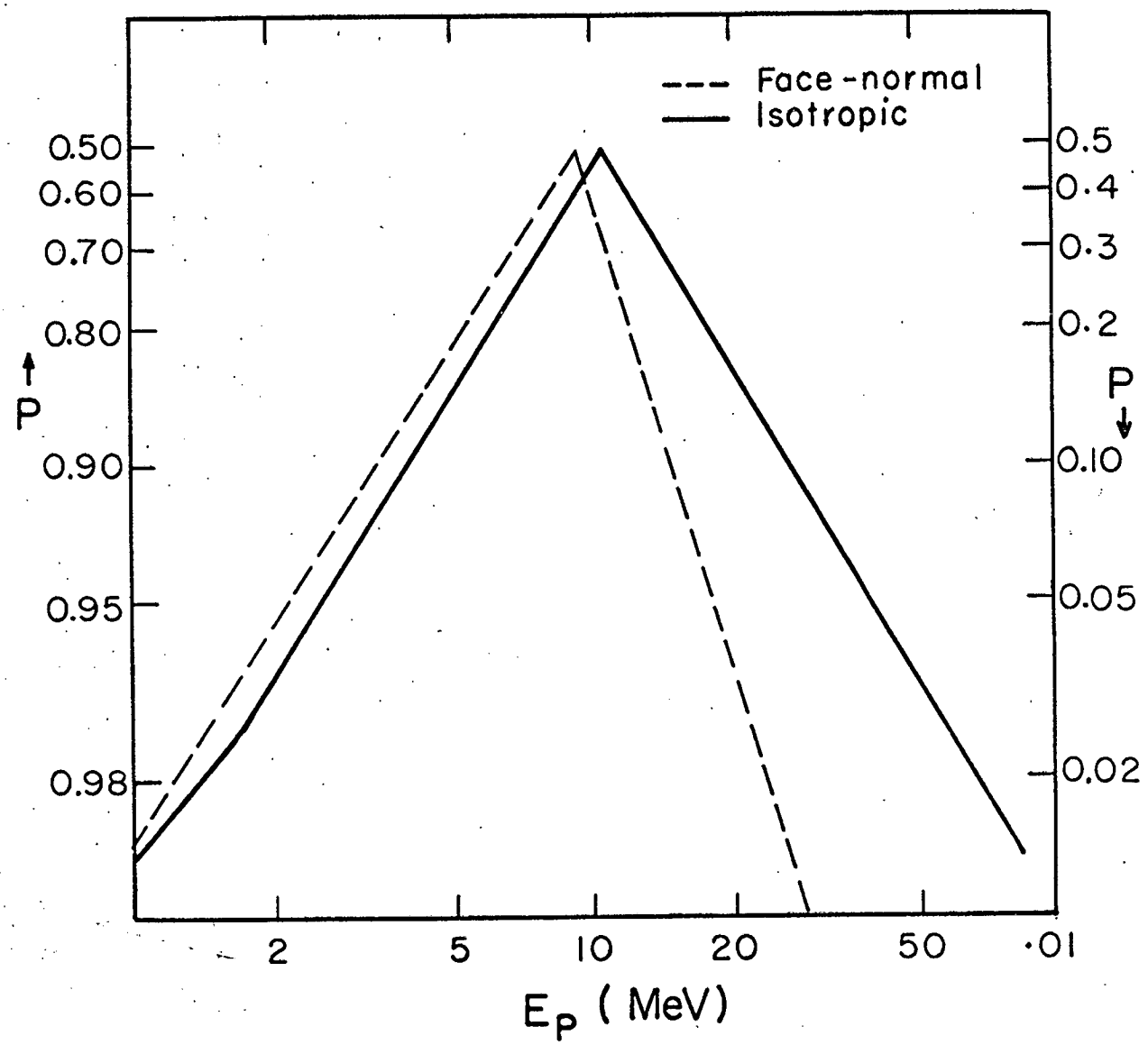

Fig. 7.

MU-26965

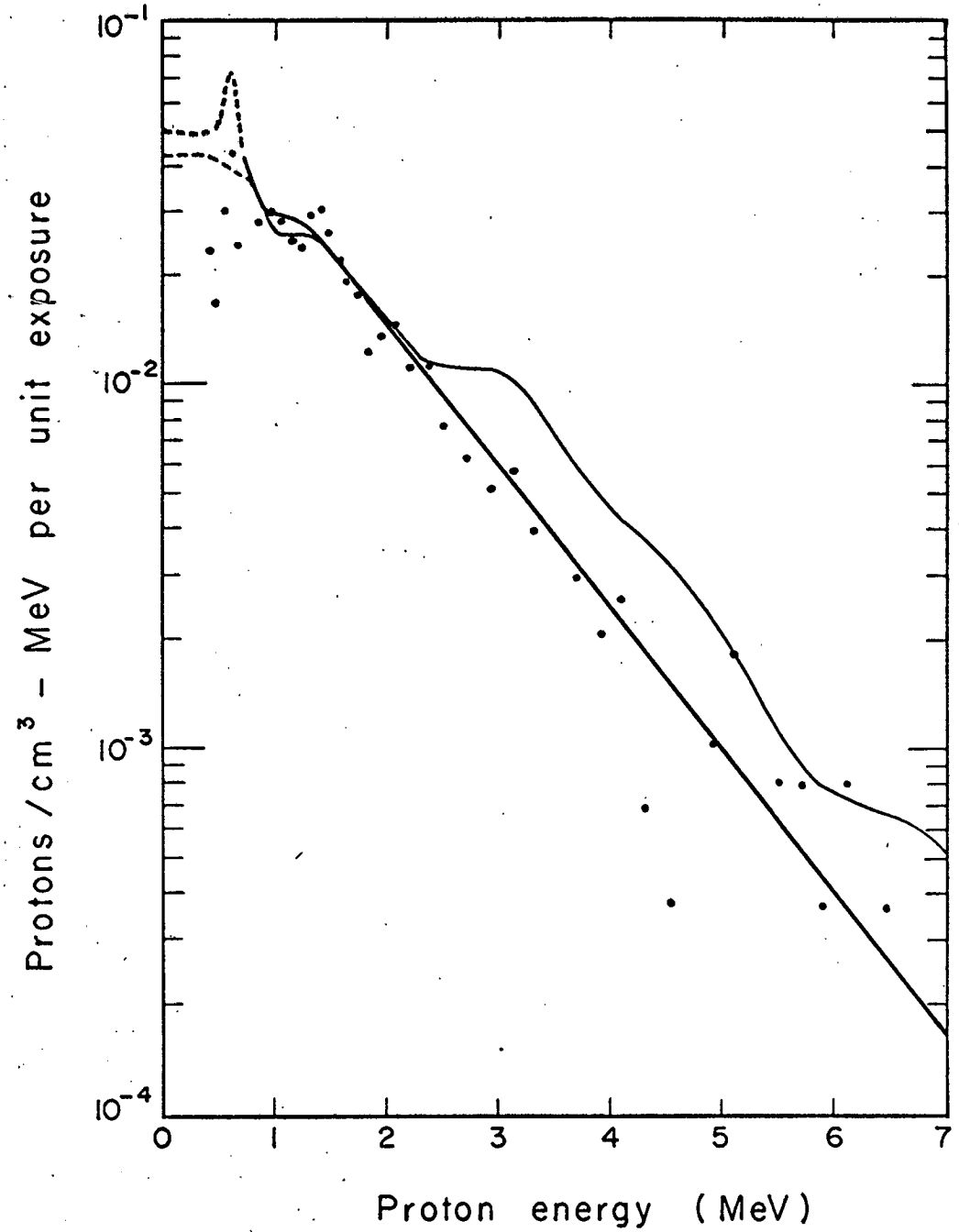

Fig. 8.

MU-26956

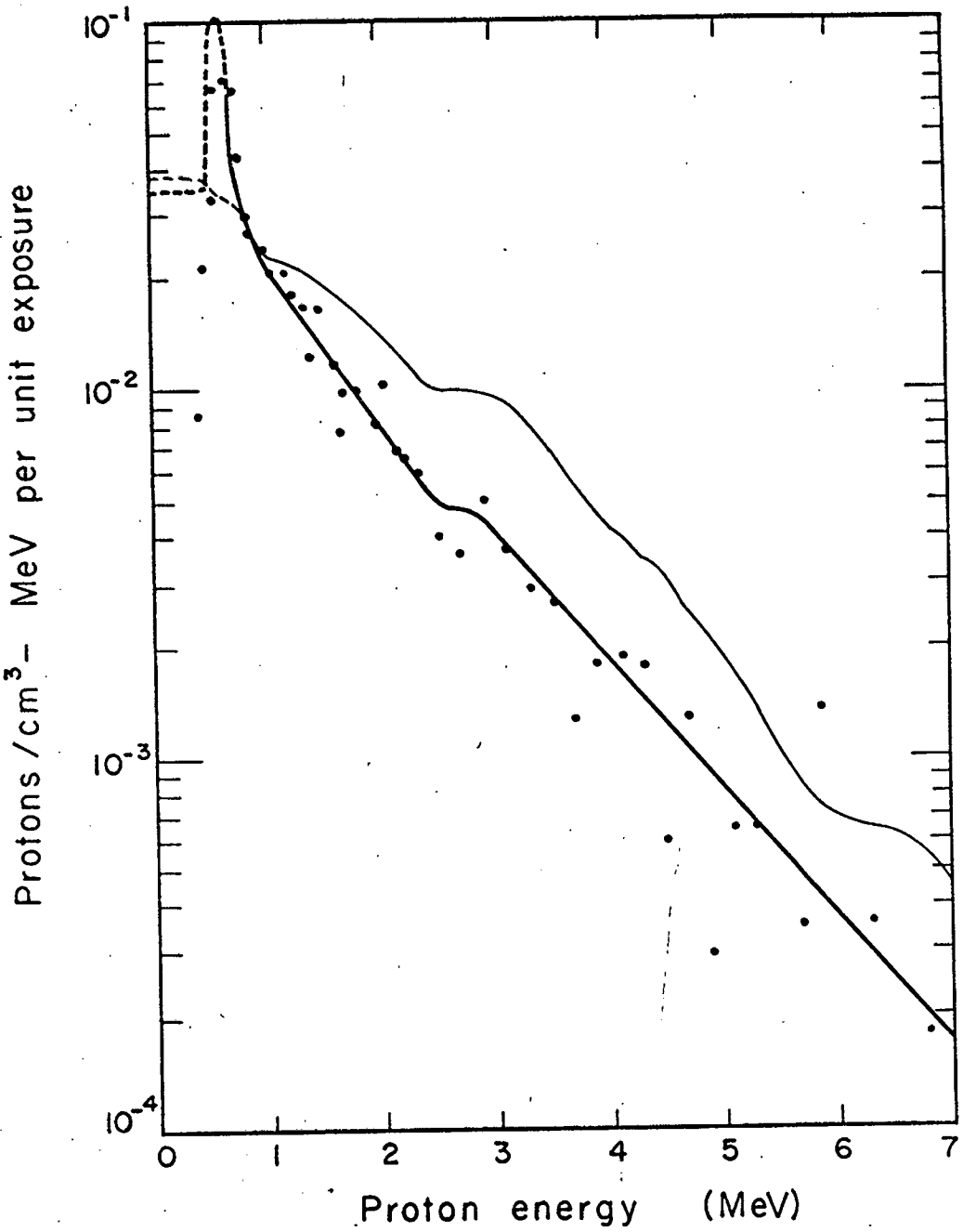

Fig. 9.

MU-26957

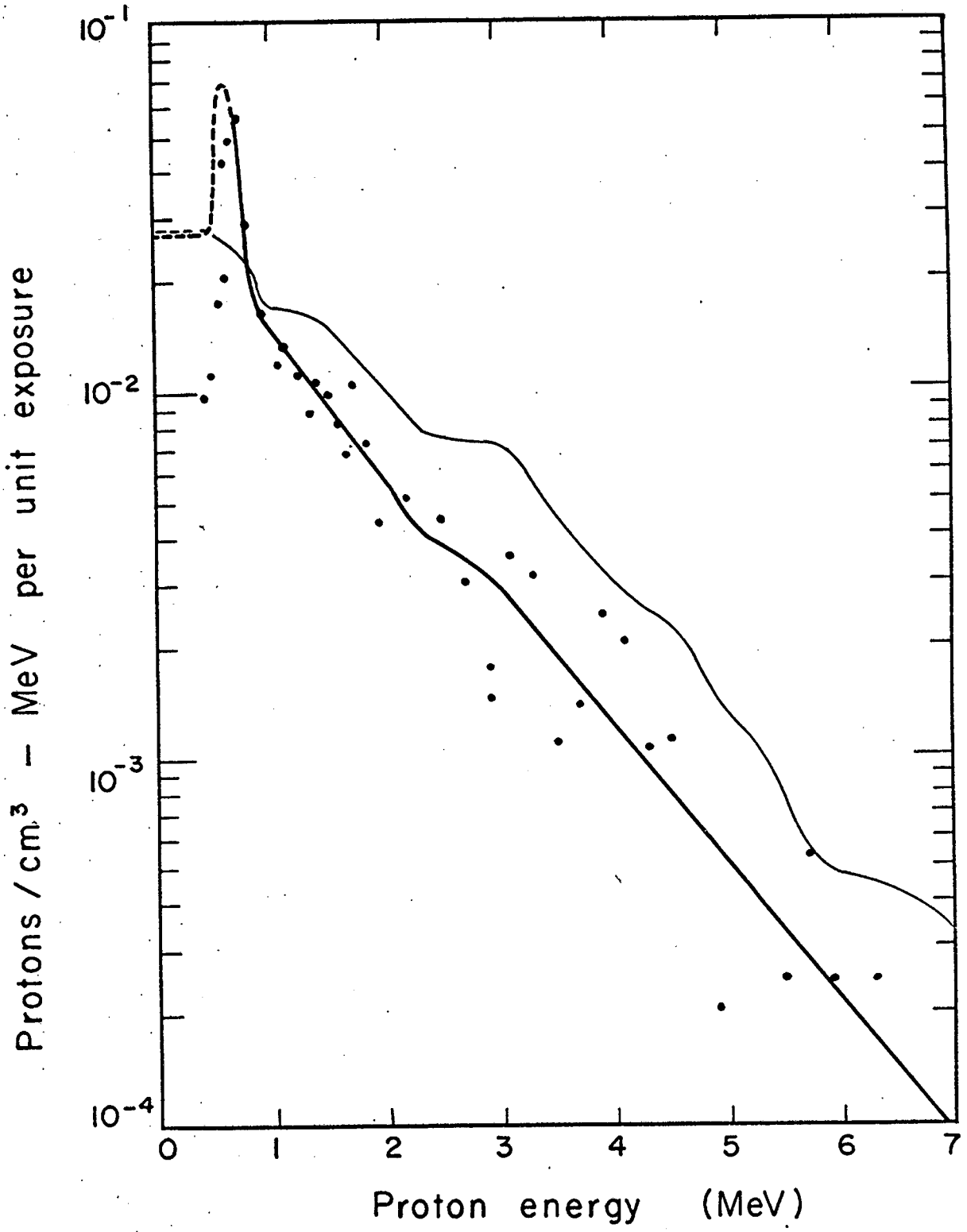

Fig. 10.

MU-26959

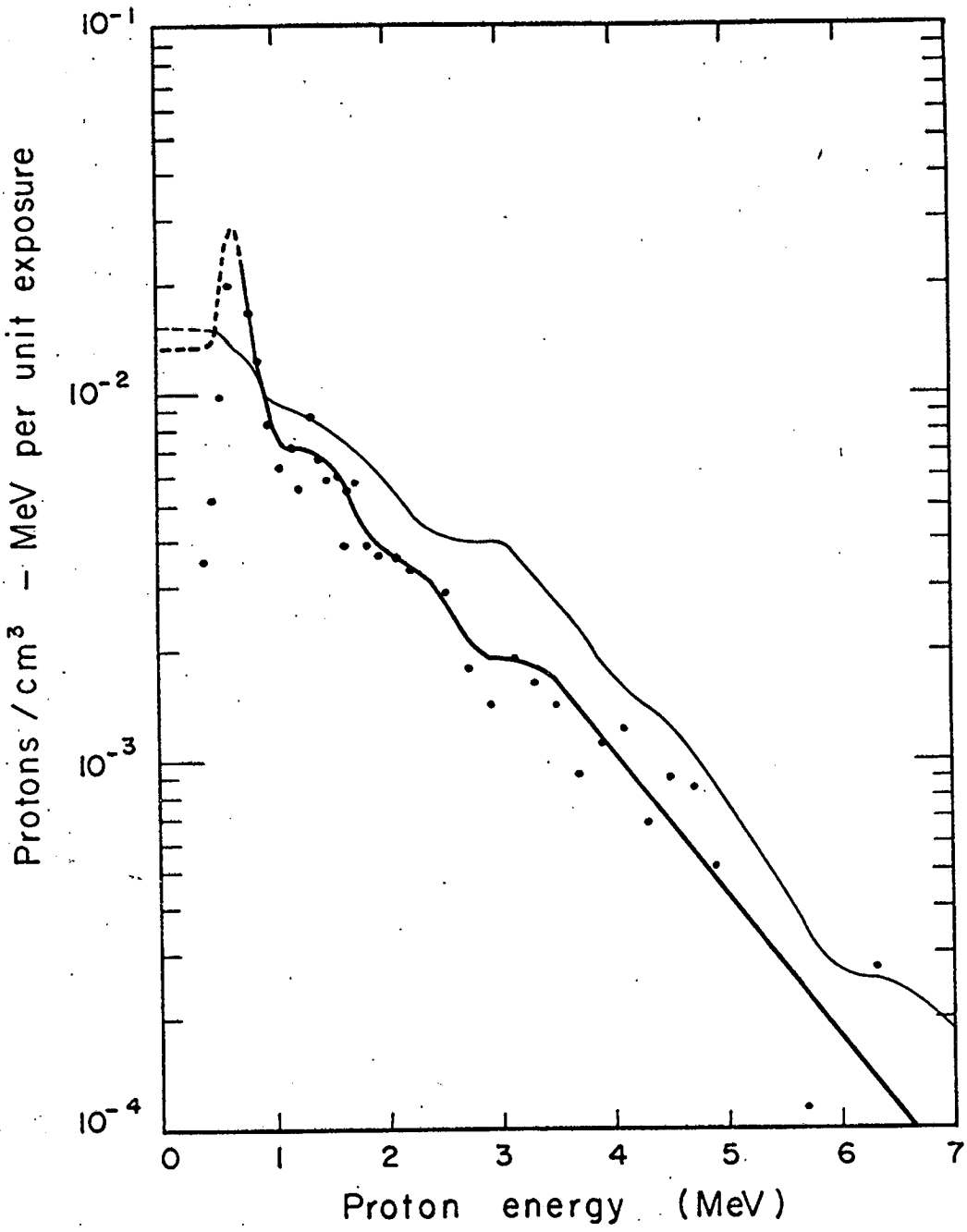

Fig. 11.

MU-26958

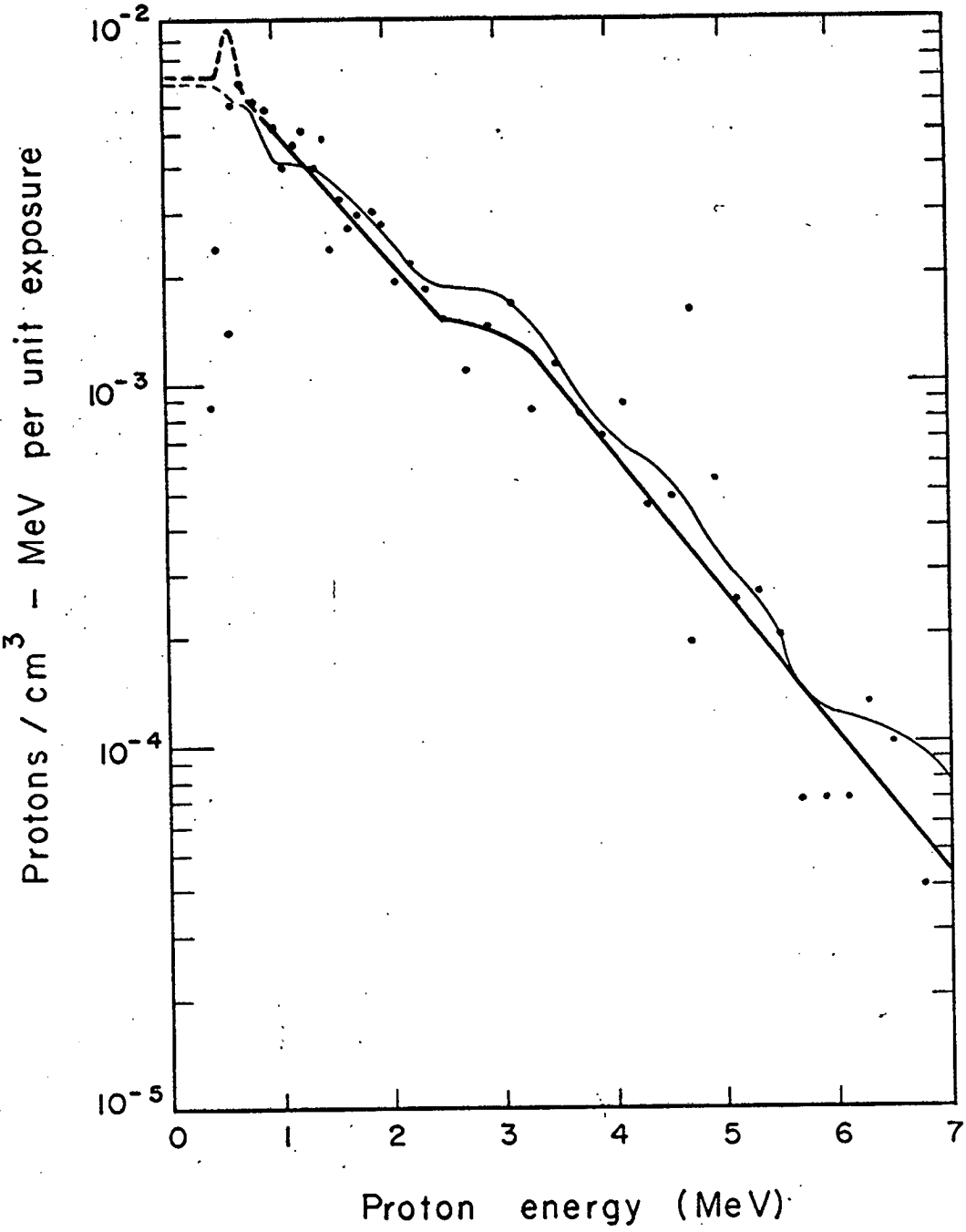

Fig. 12.

MU-26955

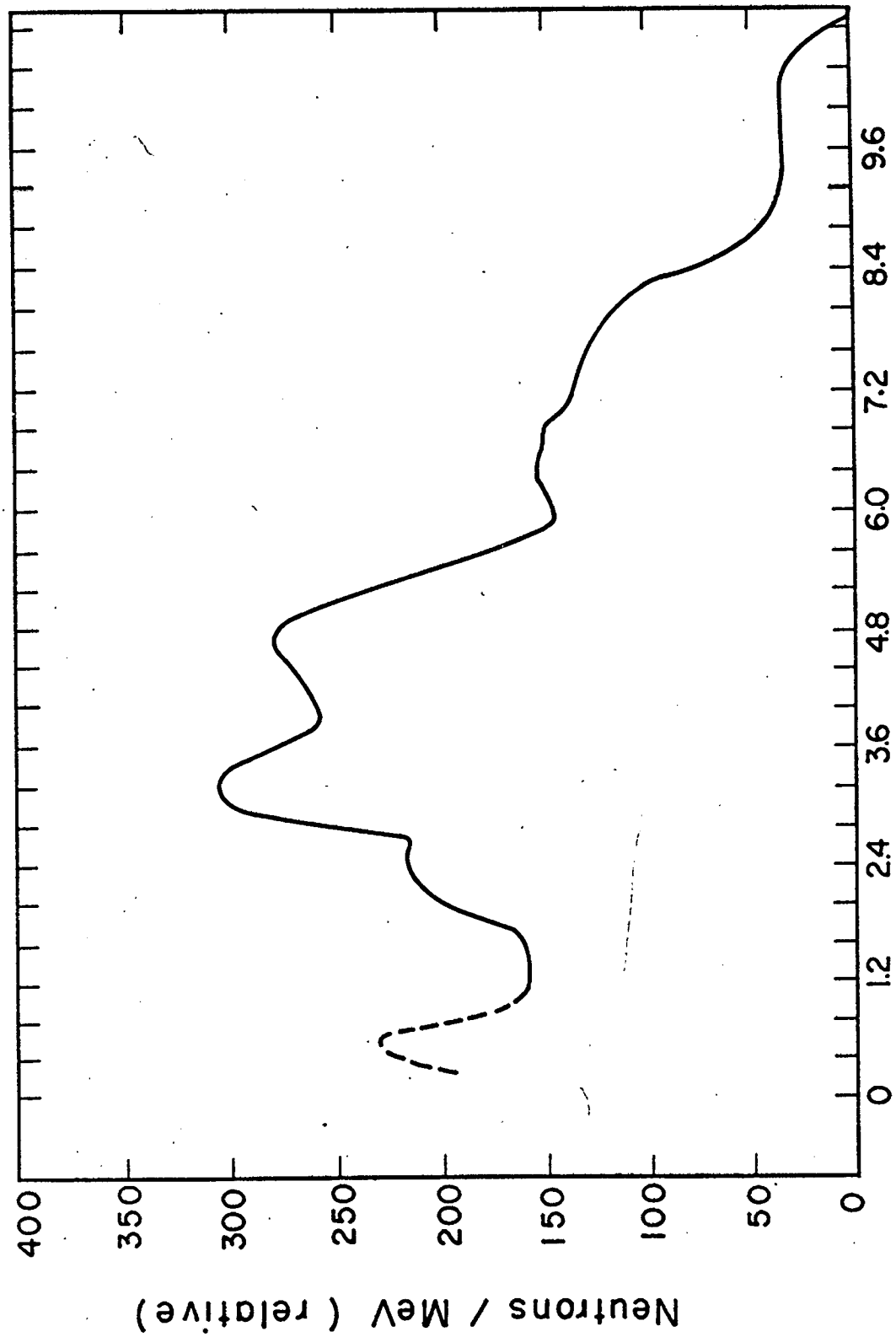
Neutrons / MeV (relative)
400
350
300
250
200
150
100
50
0
0
1.2
2.4
3.6
4.8
6.0
7.2
8.4
9.6
Neutron energy
MU-26961

Fig. 13.

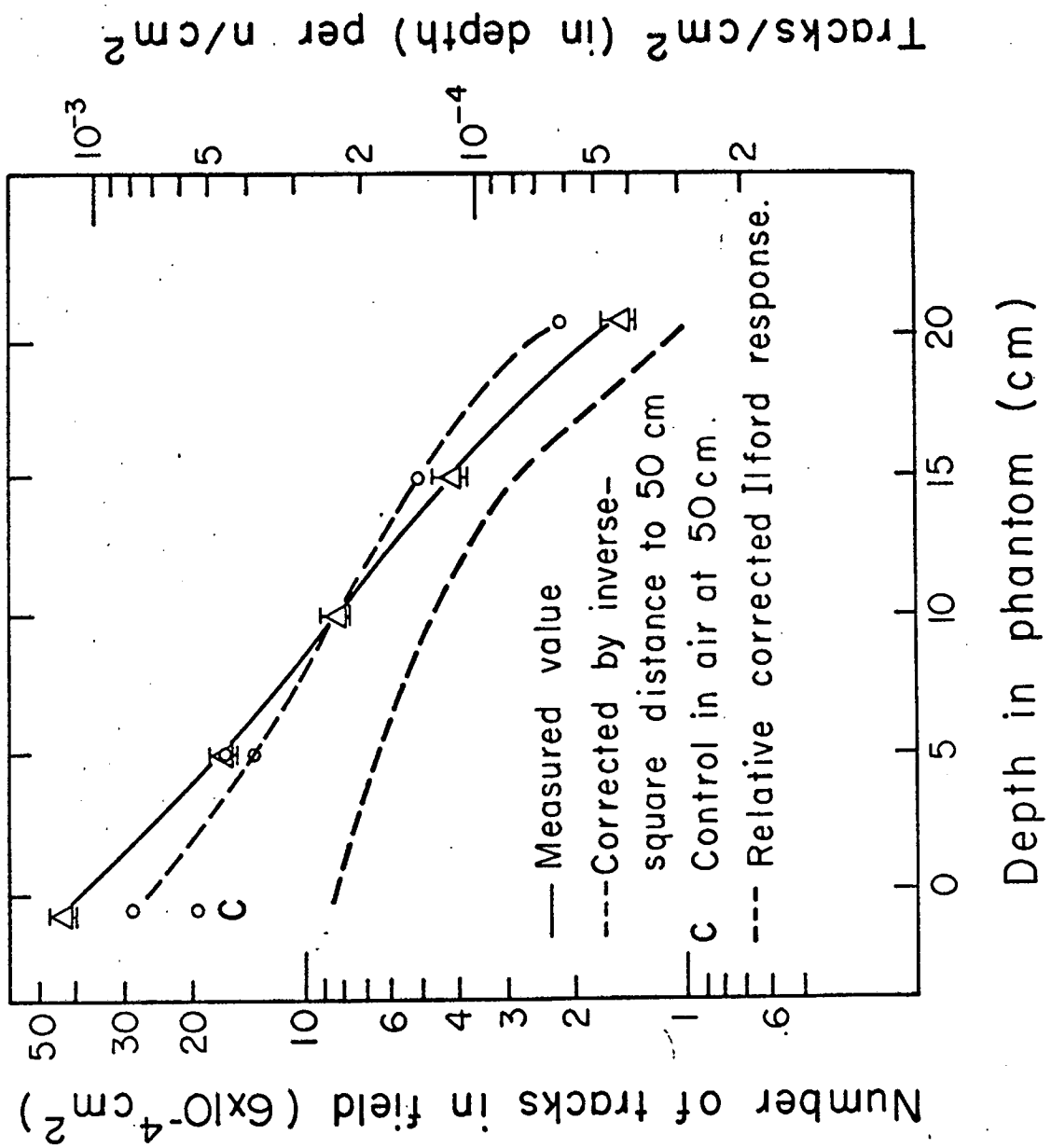
Tracks/cm² (in depth) per n/cm²
10⁻³
5
2
10⁻⁴
5
2
Number of tracks in field (6x10⁻⁴cm²)
50
30
20
10
6
4
3
2
1
.6
Depth in phantom (cm)
0
5
10
15
20
Measured value
Corrected by inverse-square distance to 50 cm
C Control in air at 50cm.
Relative corrected Ilford response.
C
C
MU-26962

Fig. 14.

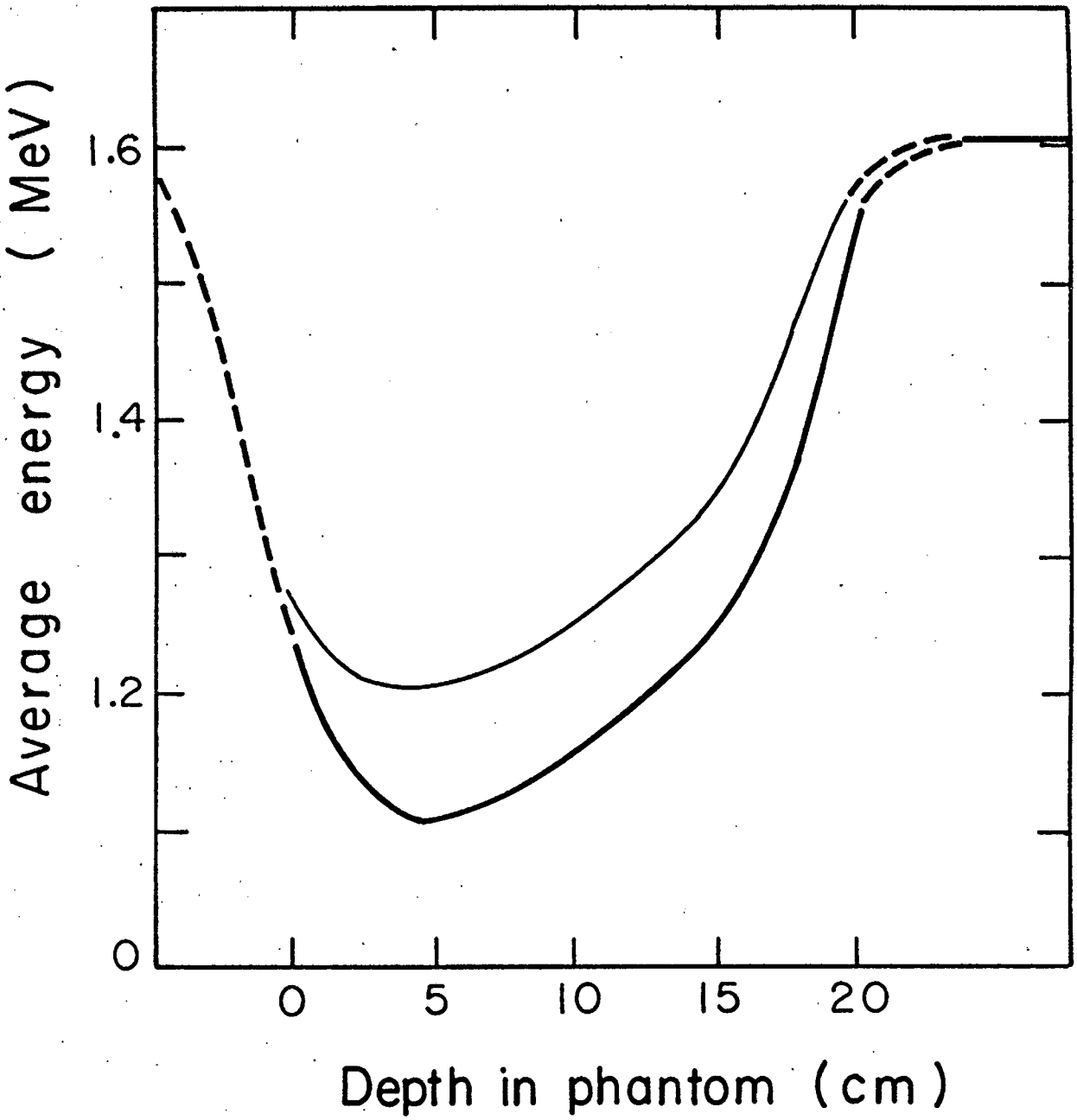

Fig. 15.

MU-26963

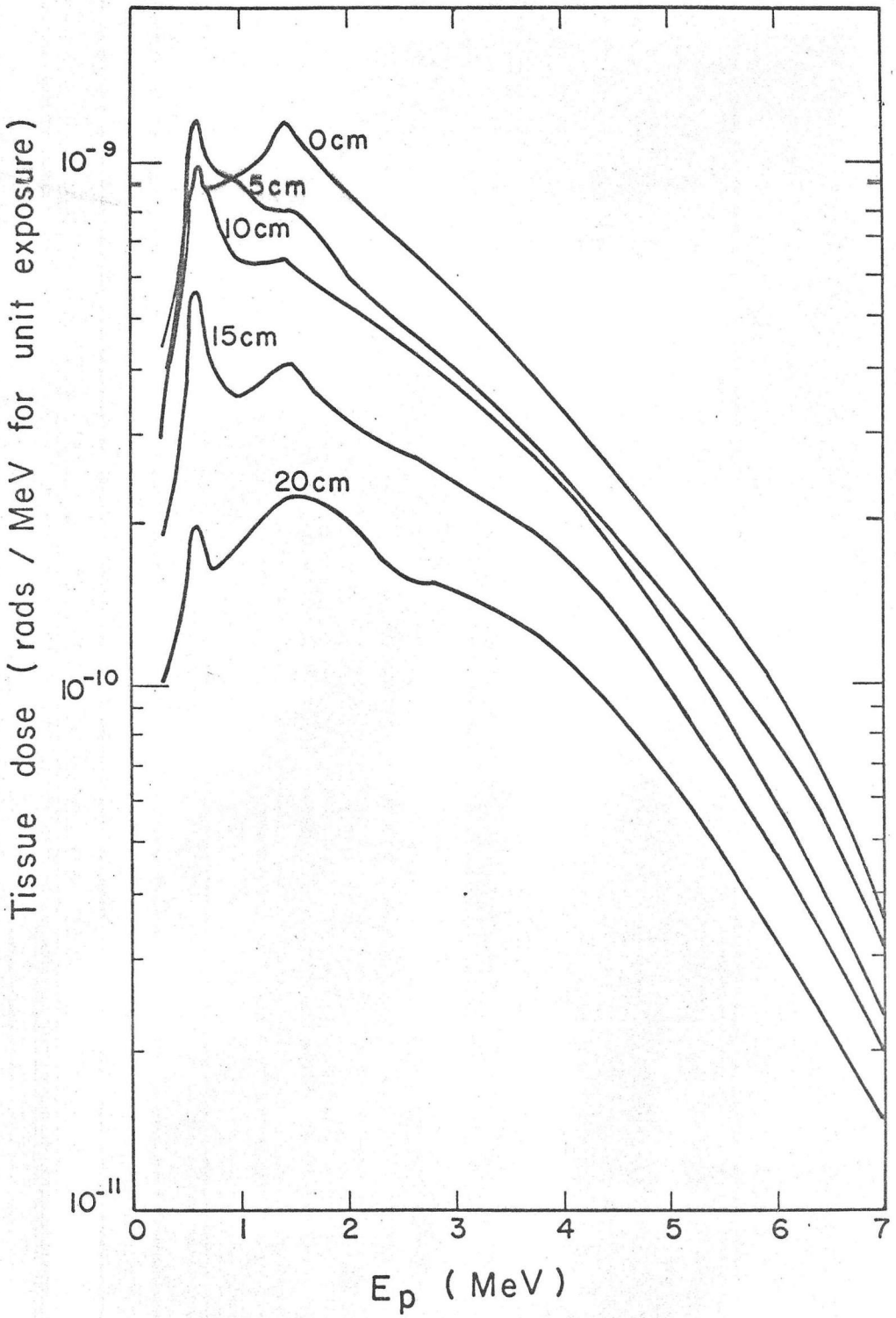

Fig. 16.

MU-26960

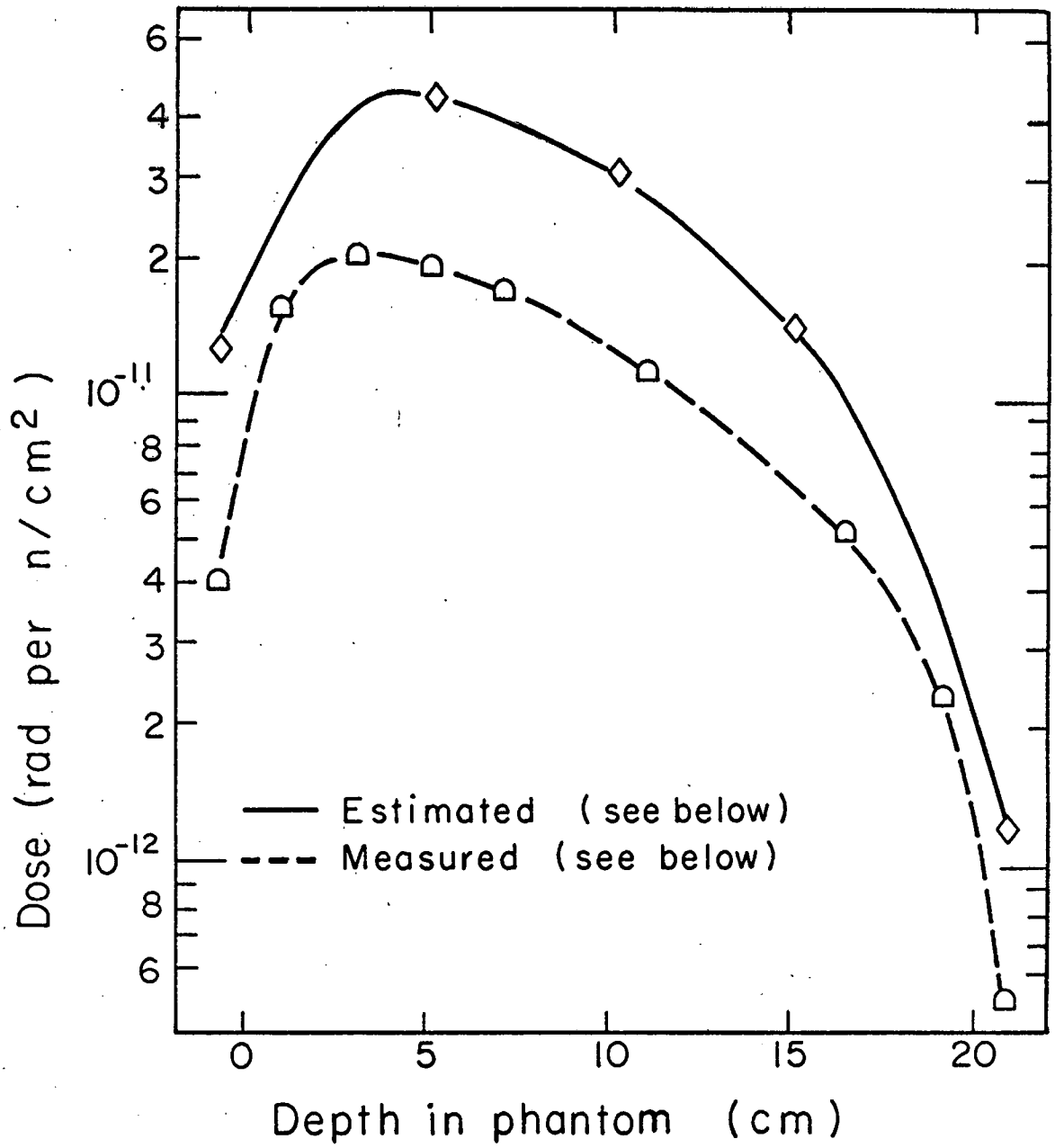

Fig. 17

MU-26964

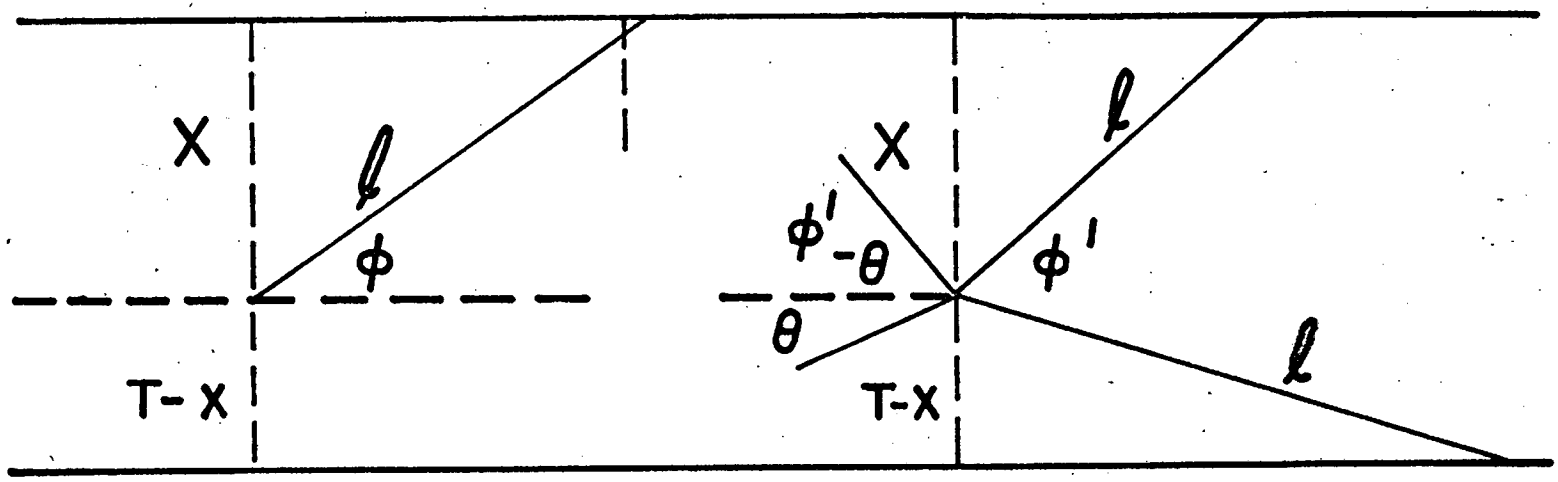

Left, case 1, face-normal exposure; right, case 2, isotropic exposure

Fig. 18.

MU-26967